

# An Rf-Gun-Driven Recirculated Linac as Injector and FEL Driver

Ake Andersson, Mikael Eriksson, Sverker Werin<sup>1</sup>  
MAX-Laboratory, University of Lund, Lund, Sweden

Sandra Biedron  
Argonne National Laboratory, Advanced Photon Source, Argonne, Illinois

Henry Freund  
Science Applications International Corporation, McLean, Virginia

RECEIVED  
OCT 12 1999  
OSTI

*A new pre-injector for the MAX-Laboratory is under design and construction. A thermionic rf gun, designed to operate at medium currents with low back bombardment power, is under construction. The gun will, via a magnetic compressor and energy filter, feed a recirculated linac consisting of two SLED-equipped structures giving 125 MeV each. The first will be delivered in 1999. The system is aimed as a pre-injector for the existing storage rings at MAX-Lab, but will also open up possibilities for a SASE FEL in the UV reaching above 100 MW below 100 nm.*

## Introduction

The injector systems at MAX-Lab are currently being upgraded. The 100-MeV racetrack microtron [1] that currently feeds the two storage rings MAX I and MAX II will be replaced by a new injector system consisting of two 5.2-m, 3-GHz acceleration sections of the DESY II type [2] and a SLED system [3]. Each section will give an energy gain of 125 MeV and the two sections will be recirculated once to give a total of 500 MeV. The linacs will be injected from a newly designed 2.3-MeV thermionic rf gun. The total circumference of this system is 30 m or 100 ns. The electron gun is equipped with a fast kicker magnet that allows a 100-ns-long electron beam to be accelerated in the linacs. Apart from being used as a storage ring injector, the injection system will also open up new possibilities for its use as an electron source for a SASE (Self-Amplified Spontaneous Emission) FEL tunable from the IR to the UV spectral regions.

## 1. THE INJECTOR

### 1.1 Rf Gun

The gun is a  $\frac{1}{2}+\frac{1}{2}+1$  cell 3-GHz structure using a 6-mm-diameter cathode and having an input coupling hole and a plunger hole in the main cavity. The gun layout is shown in Figure 1.

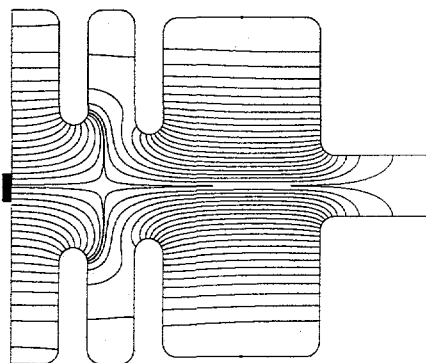


Figure 1. Gun layout (overall inner length 100 mm, maximum inner radius 40.69 mm)

<sup>1</sup>MAX-Lab, P.O. Box 118, S-221 00 Lund, Sweden. Email: sverker.werin@maxlab.lu.se Fax: 46-46-222 47 10

## **DISCLAIMER**

**This report was prepared as an account of work sponsored by an agency of the United States Government. Neither the United States Government nor any agency thereof, nor any of their employees, make any warranty, express or implied, or assumes any legal liability or responsibility for the accuracy, completeness, or usefulness of any information, apparatus, product, or process disclosed, or represents that its use would not infringe privately owned rights. Reference herein to any specific commercial product, process, or service by trade name, trademark, manufacturer, or otherwise does not necessarily constitute or imply its endorsement, recommendation, or favoring by the United States Government or any agency thereof. The views and opinions of authors expressed herein do not necessarily state or reflect those of the United States Government or any agency thereof.**

## **DISCLAIMER**

**Portions of this document may be illegible in electronic image products. Images are produced from the best available original document.**

The gun structure has been simulated using SUPERFISH [4], and the electron beam behaviour was simulated with PARMELA [5] using the fields resulting from the cavity simulations. The results are given in Table 1. The maximum fields on the gun surface stay below 100 MV/m, which is acceptable, while producing 81 MV/m on axis.

The input coupling hole size will be defined by measurements on a prototype gun. The system is designed to be over coupled in order to be self-stabilising while exposed to beam loading.

The actual coupling between the two cavities will also be measured on the prototype. This parameter is very sensitive for the precise geometry, frequency and input coupling.

Table 1. Gun Performance

Power dissipation	2.02			MW @ 81.4 MV/m on axis
Q	15030			
Shunt impedance	60.6			MΩ/m
Maximum electric field on axis	81.4			MV/m
Maximum electric field on boundary	97.4			MV/m @ 81.4 MV/m on axis
Frequency	2999.15			MHz (dependent on mesh size)
Beam kinetic energy	2.3			MeV (kinetic ⇒ 2.8 total)
Rise time	0.42			μs
Input coupling	3			
Coupling between cavities	2.64			
	0 mA	100 mA	600 mA	
Beam power	0	0.23	1.38	MW (@ dE=2.3 keV)
Energy spread	< 1	3.4	29	keV (total)
Pulse length	0.26	0.37	0.97	ps (total) ≈ deg (total)
Emittance	0.09	0.43	1.3	π mm mrad (@ E=2.8 MeV)
Emittance, norm	0.48	2.4	7.0	π mm mrad

Several parameters are shown in the next three figures: phase space diagrams in Figure 2, energy versus time distribution in Figure 3, and energy spread and bunch length in Figure 4. All values are well within specifications for the injector, but the tails in the bunch length and energy have to be removed; this will be performed by an energy filter (see below).

The emittance of the gun is strongly dependent upon space charge (Figure 2). No actual compensation is done for emittance blow-up by space charge, and thus the emittance varies with the current. The most significant effect, though, is in the longitudinal direction and acts on the energy spread (Figure 3).

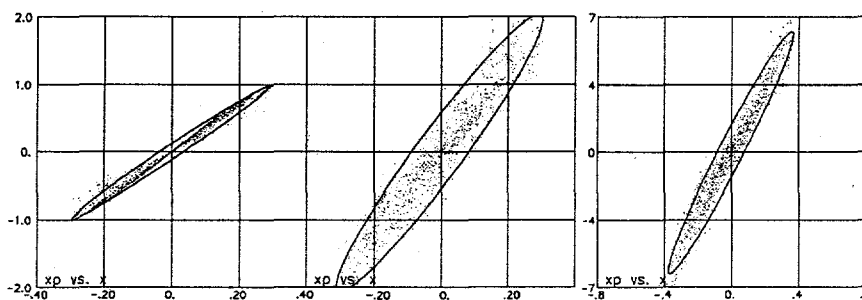


Figure 2. Phase space ( $x'$ ,  $x$ ) at the gun exit (horizontal and vertical direction are identical) for  $I = 0 / 100 / 600$  mA, respectively, at  $E_k = 2.3$  MeV ( $x$  in cm and  $x'$  in mrad)

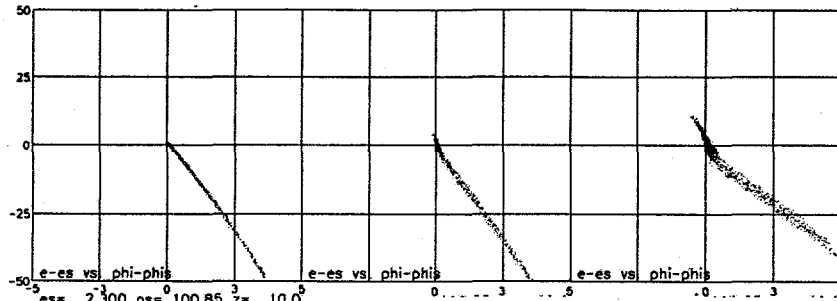


Figure 3. Energy (keV) versus phase (degrees of 3 GHz) at the gun exit ( $I = 0 / 100 / 600$  mA,  $E_k = 2.3$  MeV)

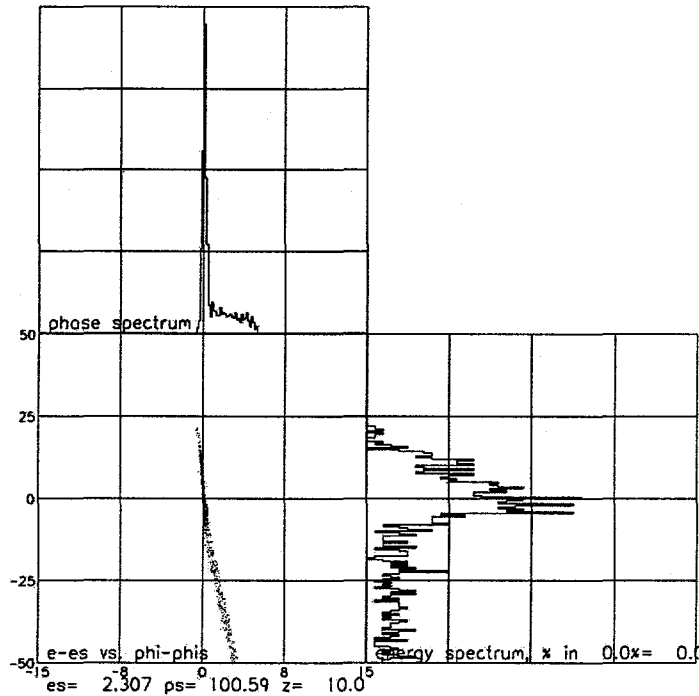


Figure 4. Energy (keV) and phase distribution (degrees of 3 GHz) at the gun exit ( $I = 600$  mA,  $E_k = 2.3$  MeV)

Tuning of the gun will initially be made by a fixed plunger in the main cell. This plunger can be removed and made smaller, thus changing the frequency, and coupling of the system. During operation, the tuning of the structure can only be made by temperature control.

YAG screens and current monitors are foreseen as diagnostics tools (Figure 5).

### 1.1.1 Rf system

The rf system should provide 2 MW for the structure and an additional 1.38 MW for the beam (600 mA gaining 2.3 MeV), for a total of 3.38 MW. The frequency of the system is 3 GHz. The klystron currently feeding the microtron has a peak power of 5 MW and 1  $\mu$ s pulse, which will suffice for operation of the gun and future development of guns running with higher energy gain and currents.

### 1.1.2 Energy filter

The bunch exiting the rf gun is too long to be fed into the linac structure, as it would simply create too large of an energy spread in the linac. Filtering of the unwanted particles should be done at the lowest possible energy to reduce radiation problems and power. Thus, a magnetic energy filter is installed between the gun and the linac entrance. This filter can also act as a compressor for the electron bunch as the energy varies along the bunch. In practise, though, this is difficult because the space charge increases energy spread and destroys the longitudinal bunch distribution.

The energy filter (Figure 5) consists of two  $60^\circ$  dipole magnets with horizontal focusing. Between the two magnets are focusing quadrupoles and a slit to provide energy filtering. The momentum compaction of the system can be fine tuned by the centre quadrupole, thus providing different compression rates.

The final data are plotted in Figures 6 and 7 and are listed in Table 2. The energy filter gives a number of operational possibilities regarding the energy window and thus the pulse length and current.

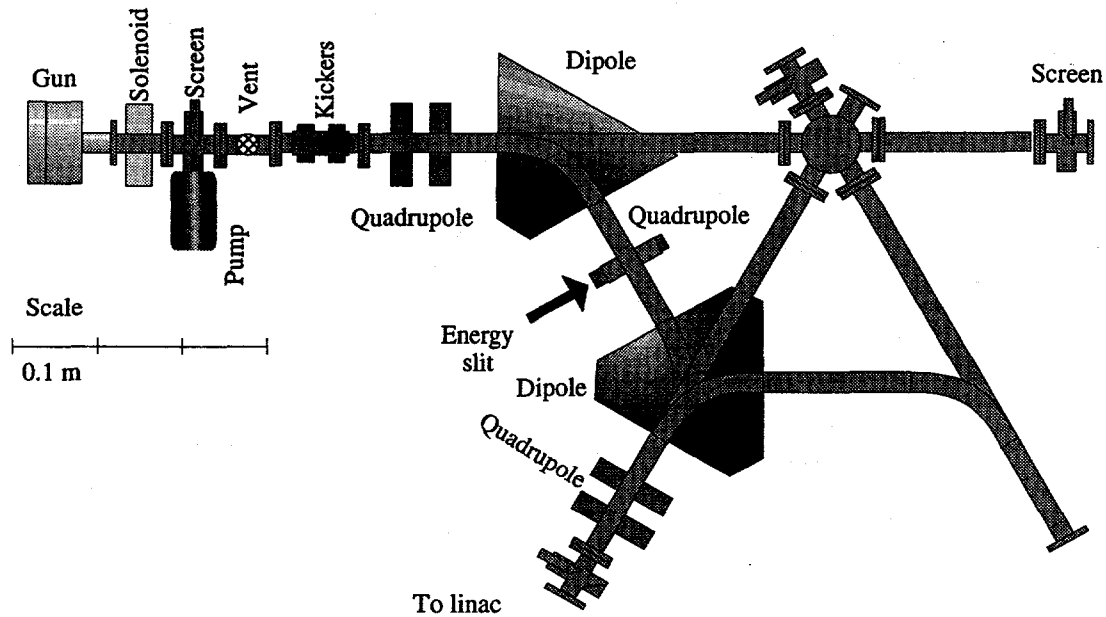


Figure 5. The energy filter and vacuum system

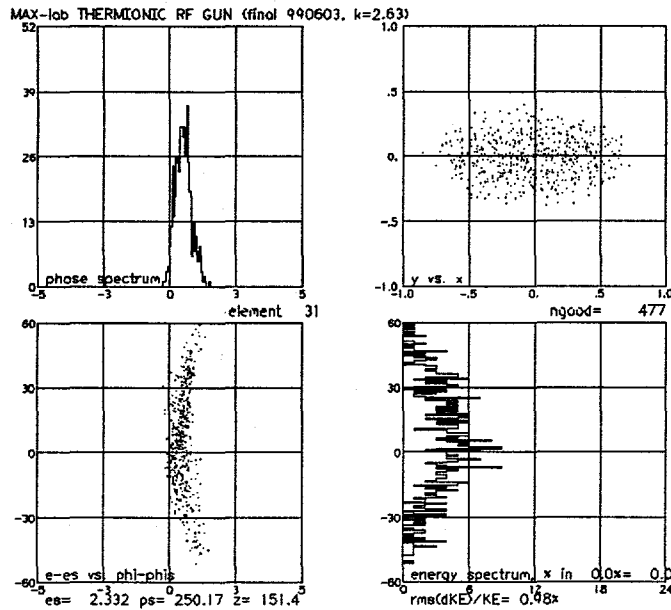


Figure 6. Energy distribution, bunch length and beam size at the linac entrance (@600 mA from gun) (x in cm, phase in deg, energy in keV)

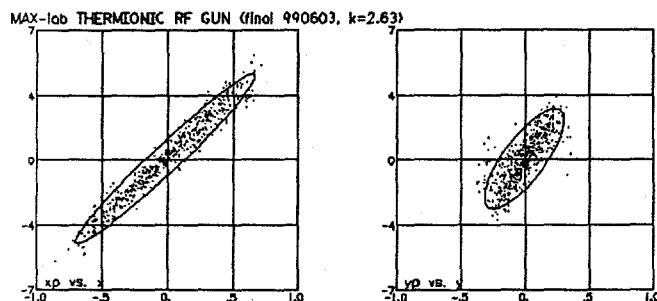


Figure 7. Phase space at the linac entrance ( $x$  in cm,  $x'$  in mrad) (@600 mA from gun) (beam not corrected to be convergent)

Table 2. Beam Parameters at Energy Filter Exit / Linac Entrance

Current	300 mA (600 mA in gun)
x-size (total)	6 mm
y-size (total)	3 mm
length (total)	2 deg (= 0.56 mm = 1.9 ps)
dE (total)	110 keV
$\epsilon_{\text{norm}}$	$8.4 \pi$ mm mrad

### 1.2 Linac

Each of the two linac sections will provide >125 MeV each (Table 3). The structures, ordered from the ACCEL company, are identical to the ones used for the SLS injector and the non-SC concept presented for TESLA [6]. The structures are of the travelling wave (TW) type and have damping material in the end cells that removes the need for an external power dump.

One naked linac structure, fed by a 35-MW klystron, can give a maximum energy gain of 77 MeV in standard configuration. Since this is insufficient, a SLED system is added to increase the beam energy by a factor of 1.8. The no-load energy gain/linac is thus 138 MeV, which drops to 120 MeV at 250-mA beam current.

Table 3. The Linac System (one structure)

Length	5.2	m
$R_{\text{sh}}$	52	M $\Omega$ /m
Q	10,000	
Damping	0.5	
Fill time	0.7	$\mu$ s
Decay time	1.38	$\mu$ s
Phase shift	3.8	$\mu$ s
Frequency	3	GHz
Klystron power	35	MW
Energy gain (no SLED, 0 A)	77.35	MeV
Energy gain (SLED, 0 A)	138.7	MeV
Energy gain (SLED, 50 mA)	136.5	MeV
Peak gradient increase by SLED	x 2.63	
Peak integrated gradient increase by SLED	x 1.793	

The linac will suffer from beam loading at higher currents, but a current of 50 mA, the desired current for the storage rings, only lowers the total energy gain from 138 MeV (0 mA) to 136.5 MeV/section. This provides the opportunity to run the klystrons below peak power, which radically increases their lifetime.

## 2. NEW POSSIBILITIES: SASE FEL IN THE VISIBLE TO ULTRAVIOLET

This new injector will allow MAX-Lab the possibility of building a single-pass FEL based on the SASE process. The recirculating linac described above will be able to drive SASE light tunable from the visible through ultraviolet wavelengths. The motivation is twofold: to perform experiments strictly with the SASE output and to provide a pump-probe method in the ultraviolet with the light produced by MAX-II when tuned to a slightly lower energy.

### 2.1 Undulators

A possible undulator design, as used in the simulations, is a near-copy of the undulators used in the low-energy undulator test line (LEUTL) project at the Advanced Photon Source at Argonne National Laboratory. These parameters are found in Table 4 [7,8].

Table 4. Undulator Parameters

On-axis undulator strength (kG)	10.06
Undulator period (cm)	3.3
K	3.1
Undulator length (m)	2.4

### 2.2 Simulations and Analysis

Using the simulated linac output and undulator parameters found in Tables 4 and 5, respectively, the SASE case was simulated using MEDUSA [9], a 3-D FEL code based on the Gauss-Hermite waveguide modes, for the maximum energy, single- and multi-pass (250- and 500-MeV) cases. The conservative set of input beam parameters, around which all parameter scans were performed, was chosen to be an emittance of  $6\pi$  mm-mrad, an energy spread of 0.025%, and a peak current of 200 A. For both cases, wavelength scans were made around the resonant condition to find the maximum gain.

Table 5. Simulation Estimates of Thermionic rf Gun and Recirculating Linac Parameters

$\Delta E/E$ (%)	0.025
$\epsilon_n$ ( $\pi$ mm-mrad)	6
$I_{pk}$ (A)	200
$\sigma_z$ (ps)	0.5
Energy (MeV)	125-500

### 2.3 250 MeV

The first case is that of a single pass through the linac, the 250-MeV case. The wavelength scan revealed maximum gain at 401.7 nm. The results for the scans varying emittance, energy spread, and peak current are plotted in Figures 8a, 9a, and 10a, respectively. Figures 8b, 9b, and 10b illustrate the effects of gain length and saturation power as functions of the respective parameter scans.

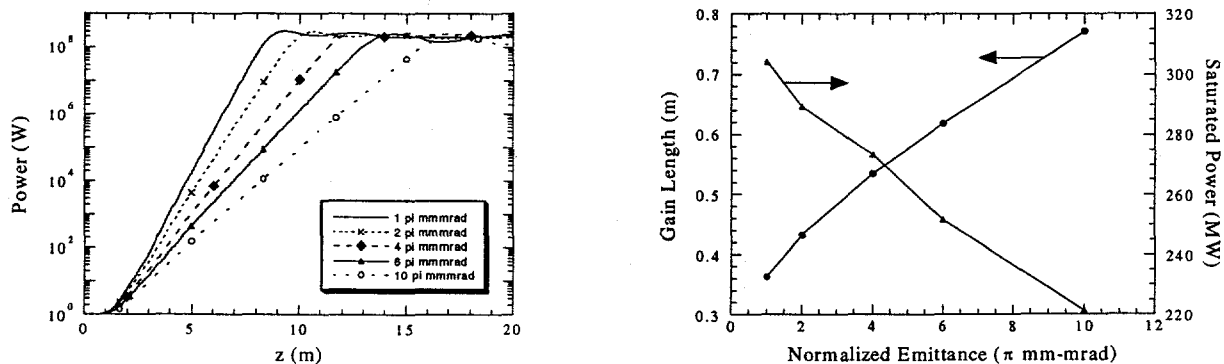


Figure 8. Emittance scans at 250 MeV,  $\Delta E/E = 0.025\%$ , and  $I_{pk} = 200$  A,

- a) power (W) versus  $z$  (m),  
 b) gain length (m) and saturated power (MW) versus  $\epsilon_n$

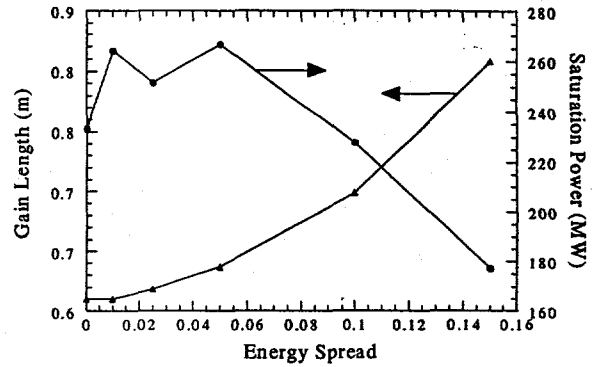
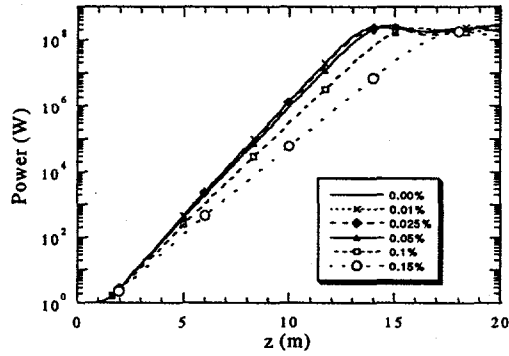


Figure 9. Energy spread scans at 250 MeV,  $\epsilon_n = 6 \pi$  mm-mrad, and  $I_{pk} = 200$  A,  
 a) power (W) versus  $z$  (m),  
 b) gain length (m) and saturated power (MW) versus  $\Delta E/E$

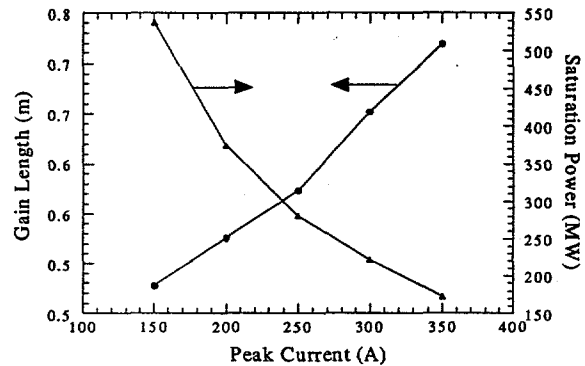
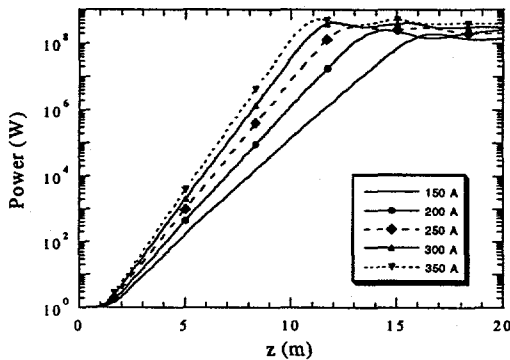


Figure 10. Peak current scans at 250 MeV,  $\epsilon_n = 6 \pi$  mm-mrad, and  $\Delta E/E = 0.025\%$ ,  
 a) power (W) versus  $z$  (m),  
 b) gain length (m) and saturated power (MW) versus  $I_{pk}$

Using the conservative set of parameters at 250 MeV, the undulator length would be required to extend 15.0 m. In the worst case, with  $\Delta E/E = 0.15\%$ ,  $\epsilon_n = 6 \pi$  mm-mrad, and  $I_{pk} = 200$  A, 18 m of undulator would be required. In the best case, with  $\epsilon_n = 1 \pi$  mm-mrad,  $\Delta E/E = 0.025\%$ , and  $I_{pk} = 200$  A, 9.3 m of undulator is required. The 250-MeV case is feasible with a maximum of eight undulators ( $\sim 20$  m), assuming the worst electron beam parameters.

## 2.4 500 MeV

The first case is that of a single pass through the linac, the 500-MeV case. The wavelength scan revealed maximum gain at 100.2 nm. The results for the scans while varying emittance, energy spread, and peak current are plotted in Figures 11a, 12a, and 13a, respectively. Figures 11b, 12b, and 13b illustrate the effects of gain length and saturation power as functions of the respective parameter scans.

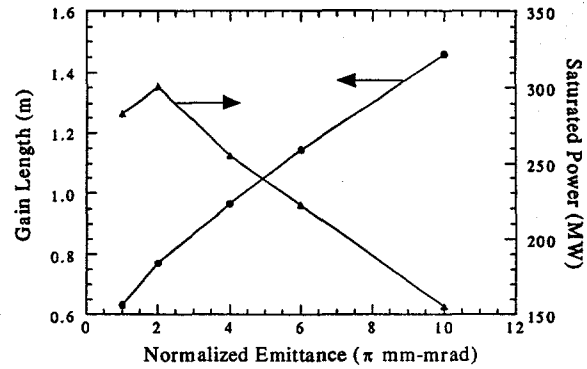
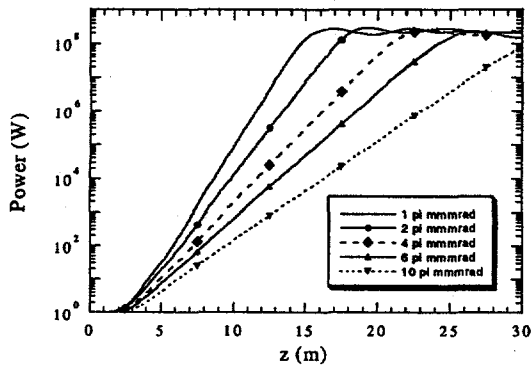


Figure 11. Emittance scans at 500 MeV,  $\Delta E/E = 0.025\%$ , and  $I_{pk} = 200$  A,  
 a) power (W) versus  $z$  (m),  
 b) gain length (m) and saturated power (MW) versus  $\epsilon_n$

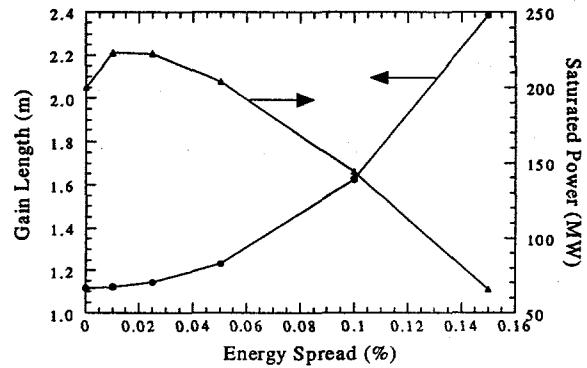
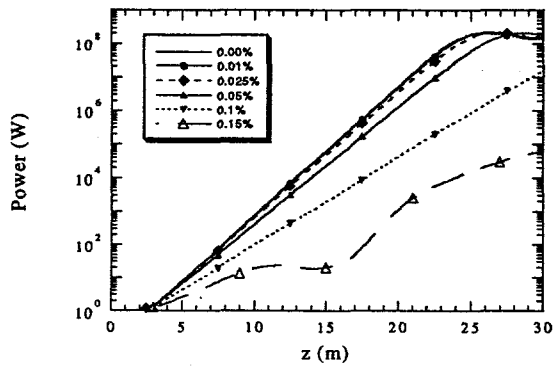


Figure 12. Energy spread scans at 500 MeV,  $\epsilon_n = 6 \pi$  mm-mrad, and  $I_{pk} = 200$  A,  
 a) power (W) versus  $z$  (m),  
 b) gain length (m) and saturated power (MW) versus  $\Delta E/E$

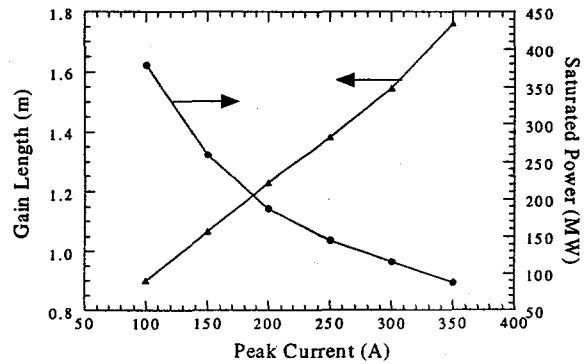
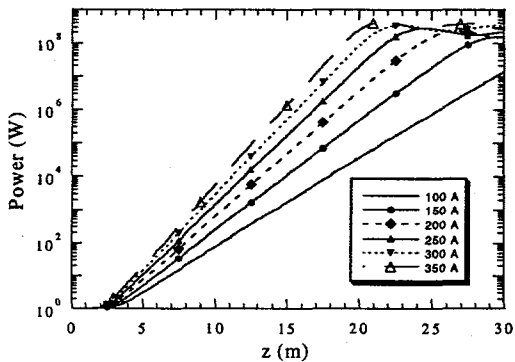


Figure 13. Peak current scans at 500 MeV,  $\epsilon_n = 6 \pi$  mm-mrad, and  $\Delta E/E = 0.025\%$ ,  
 a) power (W) versus  $z$  (m),  
 b) gain length (m) and saturated power (MW) versus  $I_{pk}$

Using the conservative set of parameters at 500 MeV, the undulator length would be required to extend 27 m. In the worst case, with  $\Delta E/E = 0.15\%$ ,  $\epsilon_n = 6 \pi$  mm-mrad, and  $I_{pk} = 200$  A, the required length of undulator would be 48 m. In the best case, with  $\Delta E/E = 0.15\%$ ,  $\epsilon_n = 1 \pi$  mm-mrad, and  $I_{pk} = 200$  A, 16 m of undulator is required. The 500-MeV case is feasible with three more undulator sections than the same length required by the 250-MeV case. For the 500-

MeV case, it would perhaps be useful to plan on variable gap undulators in order to raise K to drive saturation in a shorter z.

### 3. CONCLUSIONS

The new injector under construction at MAX-Lab will not only provide a beam for injection into the storage rings, but will also provide an intense beam as a source for an FEL in the UV. Powers above 100 MW at 100 nm seem feasible. Plans include further development of the concept of rf guns in order to achieve better control of the space-charge effects.

### 4. REFERENCES

- [1] M. Eriksson, The Accelerator System MAX, N. I. M., Volume 196 (1982).
- [2] Conceptual Design of the 500 GeV e+e- Linear Collider with Integrated X-ray Laser Facility, Vol II, DESY 1997-048.
- [3] Z. D. Farkas et al, SLED: A Method of Doubling the SLAC's Energy, SLAC-PUB-1453 (1974).
- [4] K. Halbach and R. F. Holsinger, "SUPERFISH -- A Computer Program for Evaluation of RF Cavities with Cylindrical Symmetry," Particle Accelerators 7 (4), 213-222 (1976).
- [5] Lloyd M. Young, PARMELA, Los Alamos National Laboratory, LA-UR-96-1835, 1997.
- [6] R. Brinkmann et al, Conceptual design of a 500 GeV e+e- linear collider with integrated X-ray facility, DESY 1997-048.
- [7] S.V. Milton, "The low-energy undulator test line," in *Free-Electron Laser Challenges*, Patrick G. O'Shea, Harold Bennett, Editors, Proceedings of SPIE Vol. 2988, 20-27 (1997).
- [8] E. Gluskin et al., "The Magnetic and Diagnostics Systems for the Advanced Photon Source Self-Amplified Spontaneously Emitting FEL," in NIM Proceedings of the 20<sup>th</sup> International FEL Conference (FEL98), Williamsburg, VA, USA, 1998, to be published.
- [9] H.P. Freund, Phys. Rev. E 52, 5401 (1995).